



Solar cell efficiency tables (Version 55)

Martin A. Green¹ | Ewan D. Dunlop² | Jochen Hohl-Ebinger³ | Masahiro Yoshita⁴ | Nikos Kopidakis⁵ | Anita W.Y. Ho-Baillie¹

¹ School of Photovoltaic and Renewable Energy Engineering Australian Centre for Advanced Photovoltaics, University of New South Wales, Sydney 2052, Australia

² Directorate C—Energy, Transport and Climate European Commission—Joint Research Centre, Via E. Fermi 2749, IT-21027 Ispra (VA), Italy

³ Department of Characterisation and Simulation/CalLab Cells, Fraunhofer-Institute for Solar Energy Systems, Heidenhofstr. 2, D-79110 Freiburg, Germany

⁴ Research Center for Photovoltaics (RCPV), National Institute of Advanced Industrial Science and Technology (AIST), Central 2, Umezono 1-1-1, Tsukuba, Ibaraki 305-8568, Japan

⁵ National Renewable Energy Laboratory, 15013 Denver West Parkway, Golden, Colorado 80401, USA

Correspondence

Martin A. Green, School of Photovoltaic and Renewable Energy Engineering, University of New South Wales, Sydney 2052, Australia.
Email: m.green@unsw.edu.au

Abstract

Consolidated tables showing an extensive listing of the highest independently confirmed efficiencies for solar cells and modules are presented. Guidelines for inclusion of results into these tables are outlined, and new entries since July 2019 are reviewed.

KEYWORDS

energy conversion efficiency, photovoltaic efficiency, solar cell efficiency

1 | INTRODUCTION

Since January 1993, "Progress in Photovoltaics" has published six monthly listings of the highest confirmed efficiencies for a range of photovoltaic cell and module technologies.^{1–3} By providing guidelines for inclusion of results into these tables, this not only provides an authoritative summary of the current state-of-the-art but also encourages researchers to seek independent confirmation of results and to report results on a standardised basis. In Version 33 of these tables,³ results were updated to the new internationally accepted reference spectrum (International Electrotechnical Commission IEC 60904-3, Ed. 2, 2008).

The most important criterion for inclusion of results into the tables is that they must have been independently measured by a recognised test centre listed elsewhere² (one new test centre listed in the Appendix of this issue). A distinction is made between three different eligible definitions of cell area: total area, aperture area, and designated illumination area, as also defined elsewhere² (note that, if masking is used, masks must have a simple aperture geometry, such as square,

rectangular, or circular). "Active area" efficiencies are not included. There are also certain minimum values of the area sought for the different device types (above 0.05 cm² for a concentrator cell, 1 cm² for a one-sun cell, 800 cm² for a module, and 200 cm² for a "submodule").

Results are reported for cells and modules made from different semiconductors and for subcategories within each semiconductor grouping (eg, crystalline, polycrystalline, and thin film). From Version 36 onwards, spectral response information is included (when possible) in the form of a plot of the external quantum efficiency (EQE) versus wavelength, either as absolute values or normalised to the peak measured value. Current-voltage (IV) curves have also been included where possible from Version 38 onwards. A graphical summary of progress over the first 25 years during which the tables have been published has been included in Version 51.²

Highest confirmed "one sun" cell and module results are reported in Tables 1–4. Any changes in the tables from those previously published¹ are set in bold type. In most cases, a literature reference is provided that describes either the result reported, or a similar result

TABLE 1 Confirmed single-junction terrestrial cell and submodule efficiencies measured under the global AM1.5 spectrum (1000 W/m²) at 25°C (IEC 60904-3: 2008, ASTM G-173-03 global).

Classification	Efficiency, %	Area, cm ²	V _{oc} , V	J _{sc} , mA/cm ²	Fill Factor, %	Test Centre, Date	Description
<u>Silicon</u>							
Si (crystalline cell)	26.7 ± 0.5	79.0 (da)	0.738	42.65 ^a	84.9	AIST (3/17)	Kaneka, n-type rear IBC ²⁹
Si (DS wafer cell)	23.2 ± 0.3	247.79 (t)	0.7119	41.14^b	79.3	ISFH (9/19)	Trina Solar, n-type^c
Si (thin transfer submodule)	21.2 ± 0.4	239.7 (ap)	0.687 ^c	38.50 ^{c,d}	80.3	NREL (4/14)	Solexel (35 µm thick) ³⁰
Si (thin film minimodule)	10.5 ± 0.3	94.0 (ap)	0.492 ^c	29.7 ^{c,e}	72.1	FhG-ISE (8/07)	CSG Solar (<2 µm on glass) ³¹
<u>III-V cells</u>							
GaAs (thin film cell)	29.1 ± 0.6	0.998 (ap)	1.1272	29.78 ^f	86.7	FhG-ISE (10/18)	Alta Devices ³²
GaAs (multicrystalline)	18.4 ± 0.5	4.011 (t)	0.994	23.2	79.7	NREL (11/95)	RTI, Ge substrate ³³
InP (crystalline cell)	24.2 ± 0.5 ^g	1.008 (ap)	0.939	31.15 ^a	82.6	NREL (3/13)	NREL ³⁴
<u>Thin film chalcogenide</u>							
CIGS (cell) (Cd-free)	23.35 ± 0.5	1.043 (da)	0.734	39.58 ^h	80.4	AIST (11/18)	Solar Frontier ³⁵
CdTe (cell)	21.0 ± 0.4	1.0623 (ap)	0.8759	30.25 ^d	79.4	Newport (8/14)	First Solar, on glass ³⁶
CZTSSe (cell)	11.3 ± 0.3	1.1761 (da)	0.5333	33.57 ^f	63.0	Newport (10/18)	DGIST, Korea ³⁷
CZTS (cell)	10.0 ± 0.2	1.1113 (da)	0.7083	21.77 ^a	65.1	NREL (3/17)	UNSW ³⁸
<u>Amorphous/Microcrystalline</u>							
Si (amorphous cell)	10.2 ± 0.3 ^{i,g}	1.001 (da)	0.896	16.36 ^d	69.8	AIST (7/14)	AIST ³⁹
Si (microcrystalline cell)	11.9 ± 0.3 ^g	1.044 (da)	0.550	29.72 ^a	75.0	AIST (2/17)	AIST ³⁹
<u>Peroxykite</u>							
Peroxykite (cell)	21.6 ± 0.6^{i,k}	1.0235 (da)	1.193	21.64^b	83.6	CSIRO (6/19)	ANU⁶
Peroxykite (minimodule)	17.25 ± 0.6 ^{j,l}	19.277 (da)	1.070 ^c	20.66 ^{c,m}	78.1	Newport (5/18)	Microquanta, 7 serial cells ⁴⁰
<u>Dye sensitised</u>							
Dye (cell)	11.9 ± 0.4 ⁿ	1.005 (da)	0.744	22.47 ^o	71.2	AIST (9/12)	Sharp ⁴¹
Dye (minimodule)	10.7 ± 0.4 ⁿ	26.55 (da)	0.754 ^c	20.19 ^{c,p}	69.9	AIST (2/15)	Sharp, 7 serial cells ⁴²
Dye (submodule)	8.8 ± 0.3 ⁿ	398.8 (da)	0.697 ^c	18.42 ^{c,q}	68.7	AIST (9/12)	Sharp, 26 serial cells
<u>Organic</u>							
Organic (cell)	13.45 ± 0.2^r	1.023 (da)	0.8422	23.28^b	68.6	FhG-ISE (6/19)	Uni Potsdam⁹

(Continues)

TABLE 1 (Continued)

Classification	Efficiency, %	Area, cm ²	V _{oc} , V	J _{sc} , mA/cm ²	Fill Factor, %	Test Centre, Date	Description
Organic (minimodule)	12.6 ± 0.2 ^r	26.129(da)	0.8315 ^c	21.32 ^{c,b}	71.1	FhG-ISE (9/19)	ZAE Bayern (12 cells) ¹⁰
Organic (submodule)	11.7 ± 0.2 ^r	203.98 (da)	0.8177 ^c	20.68 ^{c,b}	69.3	FhG-ISE (10/19)	ZAE Bayern (33 cells) ¹⁰

AlST, Japanese National Institute of Advanced Industrial Science and Technology; (ap), aperture area; a-Si, amorphous silicon/hydrogen alloy; CIGS, CuIn_{1-y}Ga_ySe₂; CZTS, Cu₂ZnSnS₄; CZTSSe, Cu₂ZnSnS_{4-y}Se_y; (da), designated illumination area; DS, directionally solidified (including mono cast and multicrystalline); FhG-ISE, Fraunhofer Institut für Solare Energiesysteme; nc-Si, nanocrystalline or microcrystalline silicon; (t), total area.

^aSpectral response and current-voltage curve reported in Version 50 of these tables.

^bSpectral response and current-voltage curve reported in the present version of these tables.

^cReported on a "per cell" basis.

^dSpectral responses and current-voltage curve reported in Version 45 of these tables.

^eRecalibrated from original measurement.

^fSpectral response and current-voltage curve reported in the Version 53 of these tables.

^gNot measured at an external laboratory.

^hSpectral response and current-voltage curve reported in Version 54 of these tables.

ⁱStabilised by 1000-hour exposure to 1 sun light at 50 °C.

^jInitial performance. References 7 and 8 review the stability of similar devices.

^kAverage of forward and reverse sweeps at 150 mV/s (hysteresis ± 0.26%).

^lMeasured using 13-point IV sweep with constant bias until data constant at 0.05% level.

^mSpectral response and current-voltage curve reported in Version 52 of these tables.

ⁿInitial efficiency. Reference 21 reviews the stability of similar devices.

^oSpectral response and current-voltage curve reported in Version 41 of these tables.

^pSpectral response and current-voltage curve reported in Version 46 of these tables.

^qSpectral response and current-voltage curve reported in Version 43 of these tables.

^rInitial performance. References 11 and 12 review the stability of similar devices.

TABLE 2 “Notable Exceptions” for single-junction cells and submodules: “Top dozen” confirmed results, not class records, measured under the global AM1.5 spectrum (1000 Wm⁻²) at 25°C (IEC 60904-3: 2008, ASTM G-173-03 global)

Classification	Efficiency, %	Area, cm ²	V _{oc} , V	J _{sc} , mA/cm ²	Fill Factor, %	Test Centre, Date	Description
Cells (silicon)							
Si (crystalline)	26.0 ± 0.5	4.015 (da)	0.7323	42.05^a	82.3	FhG-ISE (11/19)	FhG-ISE, p-type top/rear contacts⁴³
Si (crystalline)	25.8 ± 0.5 ^b	4.008 (da)	0.7241	42.87 ^c	83.1	FhG-ISE (7/17)	FhG-ISE, n-type top/rear contacts ⁴⁴
Si (crystalline)	26.1 ± 0.3 ^b	3.9857 (da)	0.7266	42.62 ^d	84.3	ISFH (2/18)	ISFH, p-type rear IBC ⁴⁵
Si (large crystalline)	25.1 ± 0.4	244.45 (t)	0.7470	39.55^a	85.0	ISFH (9/19)	Hanergy, n-type top/rear contacts⁴³
Si (large crystalline)	26.6 ± 0.5	179.74 (da)	0.7403	42.5 ^e	84.7	FhG-ISE (11/16)	Kaneka, n-type rear IBC ²⁹
Si (DS wafer)	22.8 ± 0.3	246.7 (t)	0.6871	40.90^a	81.2	ISFH (9/19)	Canadian Solar, p-type PERC¹⁴
Cells (III-V)							
GalnP	22.0 ± 0.3 ^b	0.2502 (ap)	1.4695	16.63 ^f	90.2	NREL (1/19)	NREL, rear HJ, strained AlnP ⁴⁶
Cells (chalcogenide)							
CdTe (thin-film)	22.1 ± 0.5	0.4798 (da)	0.8872	31.69 ⁱ	78.5	Newport (11/15)	First Solar on glass ⁴⁷
CZTSSe (thin-film)	12.6 ± 0.3	0.4209 (ap)	0.5134	35.21 ^g	69.8	Newport (7/13)	IBM solution grown ⁴⁸
CZTS (thin-film)	11.0 ± 0.2	0.2339(da)	0.7306	21.74 ^e	69.3	NREL (3/17)	UNSW on glass ⁴⁹
Cells (other)							
PeroVskite (thin-film)	25.2 ± 0.8 ^{k,l}	0.0937 (ap)	1.1805	24.14 ^a	84.8	Newport (7/19)	KRICT/MIT ¹⁵
Organic (thin-film)	17.35 ± 0.2 ^k	0.032 (da)	0.862	25.83 ^a	78.0	NREL (10/19)	SJTU/UMass ¹⁹
Dye sensitised	12.25 ± 0.4 ^{j,l}	0.0963 (ap)	1.0203	15.17 ^a	79.1	Newport (8/19)	EPFL ²⁰

AST, Japanese National Institute of Advanced Industrial Science and Technology; (ap), aperture area; CIGSSe, CuInGaSe_x; CZTSSe, Cu₂ZnSnS₄; CZTS, Cu₂ZnSn_{2-y}Se_y; (da), designated illumination area; DS, directionally solidified (including mono cast and multicrystalline); FhG-ISE, Fraunhofer-Institut für Solare Energiesysteme; ISFH, Institute for Solar Energy Research, Hamelin; NREL, National Renewable Energy Laboratory; (t), total area.

^aSpectral response and current-voltage curves reported in present version of these tables.

^bNot measured at an external laboratory

^cSpectral response and current-voltage curves reported in Version 51 of these tables.

^dSpectral response and current-voltage curve reported in Version 52 of these tables.

^eSpectral response and current-voltage curves reported in Version 50 of these tables.

^fSpectral response and current-voltage curve reported in Version 54 of these tables.

^gSpectral response and/or current-voltage curves reported in Version 46 of these tables.

^hSpectral response and current-voltage curves reported in Version 44 of these tables.

ⁱStability not investigated. References 7 and 8 document stability of similar devices.

^jMeasured using 10-point IV sweep with constant voltage bias until current determined as unchanged.

^kLong-term stability not investigated. References 11 and 12 document stability of similar devices.

^lLong-term stability not investigated. Reference 21 documents stability of similar devices.

TABLE 3 Confirmed multiple-junction terrestrial cell and submodule efficiencies measured under the global AM1.5 spectrum (1000 W/m²) at 25°C (IEC 60904-3; 2008, ASTM G-173-03 global)

Classification	Efficiency, %	Area, cm ²	Voc, V	J _{sc} , mA/cm ²	Fill Factor, %	Test Centre, Date	Description
III-V Multijunctions							
Five junction cell (bonded) (2.17/1.68/1.40/1.06/.73 eV)	38.8 ± 1.2	1.021 (ap)	4.767	9.564	85.2	NREL (7/13)	Spectrolab, 2-terminal ⁵⁰
InGaP/GaAs/InGaAs	37.9 ± 1.2	1.047 (ap)	3.065	14.27 ^a	86.7	AIST (2/13)	Sharp, 2 term. ⁵¹
GalnP/GaAs (monolithic)	32.8 ± 1.4	1.000 (ap)	2.568	14.56 ^b	87.7	NREL (9/17)	LG Electronics, 2 term.
Multijunctions with c-Si							
GalnP/GaAs/Si (mech. stack)	35.9 ± 0.5 ^c	1.002 (da)	2.52/0.681	13.6/11.0	87.5/78.5	NREL (2/17)	NREL/CSEM/EPFL, 4-term. ⁵²
GalnP/AlGaAs/Si (wafer bonded)	34.1 ± 1.2 ^c	3.987 (ap)	3.177	12.4 ^d	86.4	FhG-ISE (8/19)	Fraunhofer ISE, 2-term. ²²
GalnP/GaAs/Si (monolithic)	24.3 ± 0.9 ^c	3.987 (ap)	2.662	12.2 ^d	74.5	FhG-ISE (6/19)	Fraunhofer ISE, 2-term. ²³
GaAs/P/Si (monolithic)	20.1 ± 1.3 ^c	3.940 (ap)	1.673	14.94 ^e	80.3	NREL (5/18)	OSU/SolarAero/UNSW, 2-term. ⁵³
GaAs/Si (mech. stack)	32.8 ± 0.5 ^c	1.003 (da)	1.09/0.683	28.9/11.1 ^e	85.0/79.2	NREL (12/16)	NREL/CSEM/EPFL, 4-term. ⁵²
Perovskite/Si (monolithic)	28.0 ± 0.7 ^f	1.030 (da)	1.802	19.75 ^g	78.7	NREL (12/18)	Oxford PV ⁵⁴
GalnP/GaInAs/Ge; Si (spectral split minimodule)	34.5 ± 2.0	27.83 (ap)	2.66/0.65	13.1/9.3	85.6/79.0	NREL (4/16)	UNSW/Azur/Trina, 4-term. ⁵⁵
Other Multijunctions							
PeroVskite/CIGS	23.3 ± 0.8 ^f	1.035 (da)	1.683	19.17 ^d	72.1	FhG-ISE (6/19)	HZB, 2-term. ²⁴
a-Si/nc-Si/nc-Si (thin-film)	14.0 ± 0.4 ^{h,c}	1.045 (da)	1.922	9.94 ⁱ	73.4	AIST (5/16)	AIST, 2-term. ⁵⁶
a-Si/nc-Si (thin-film cell)	12.7 ± 0.4 ^{h,c}	1.000(da)	1.342	13.45 ^j	70.2	AIST (10/14)	AIST, 2-term. ⁵⁷
"Notable Exceptions"							
GalnP/GaAs/GaInAs	37.8 ± 1.4	0.998 (ap)	3.013	14.60 ^k	85.8	NREL (1/18)	Microlink (ELO) ⁵⁸
6 junction (monolithic) (2.19/1.76/1.45/1.19/.97/.7 eV)	39.2 ± 3.2 ^c	0.247 (ap) ^l	5.549	8.457 ^g	83.5	NREL (11/18)	NREL, inv. m'morphic ⁵⁹

AIST, Japanese National Institute of Advanced Industrial Science and Technology; (ap), aperture area; a-Si, amorphous silicon/hydrogen alloy; (da), designated illumination area; FhG-ISE, Fraunhofer Institut für Solare Energiesysteme; nc-Si, nanocrystalline or microcrystalline silicon; (t), total area.

^aSpectral response and current-voltage curve reported in Version 42 of these tables.

^bSpectral response and current-voltage curve reported in the Version 51 of these tables.

^cNot measured at an external laboratory.

^dSpectral response and current-voltage curve reported in the present version of these tables.

^eSpectral response and current-voltage curve reported in Version 52 of these tables.

^fInitial efficiency. References 7 and 8 review the stability of similar perovskite-based devices.

^gSpectral response and current-voltage curve reported in the present version of these tables.

^hStabilised by 1000-hour exposure to 1 sun light at 50 °C.

ⁱSpectral response and current-voltage curve reported in Version 49 of these tables.

^jSpectral responses and current-voltage curve reported in Version 45 of these tables.

^kSpectral response and current-voltage curve reported in Version 53 of these tables.

^lArea too small to qualify as outright class record.

TABLE 4 Confirmed terrestrial module efficiencies measured under the global AM1.5 spectrum (1000 W/m^2) at a cell temperature of 25°C (IEC 60904-3: 2008, ASTM G-173-03 global)

Classification	Effic., %	Area, cm^2	V_{oc} , V	I_{sc} , A	FF, %	Test Centre, Date	Description
Si (crystalline)	24.4 ± 0.5	13 177 (da)	79.5	5.04 ^a	80.1	AIST (9/16)	Kaneka (108 cells) ²⁹
Si (DS wafer)	20.4 ± 0.3	14 818 (ap)	39.90	9.833^b	77.2	FhG-ISE (10/19)	Hanwha Q Cells (60 cells)²⁵
GaAs (thin-film)	25.1 ± 0.8	866.45 (ap)	11.08	2.303 ^c	85.3	FhG-ISE (11/17)	Alta Devices ⁶⁰
CIGS (Cd-free)	19.2 ± 0.5	841 (ap)	48.0	0.456 ^c	73.7	AIST (1/17)	Solar Frontier (70 cells) ⁶¹
CdTe (thin-film)	19.0 ± 0.9	23 573 (da)	227.8	2.560^b	76.6	FhG-ISE (9/19)	First Solar²⁶
a-Si/nc-Si (tandem)	$12.3 \pm 0.3^{\text{d}}$	14 322 (t)	280.1	0.902 ^e	69.9	ESTI (9/14)	TEL Solar, Trubbach Labs ⁶²
Perovskite	$16.1 \pm 0.5^{\text{f}}$	802 (da)	57.3	0.3207^b	70.3	AIST (5/19)	Panasonic (55 cells)²⁷
Organic	$8.7 \pm 0.3^{\text{g}}$	802 (da)	17.47	0.569 ^h	70.4	AIST (5/14)	Toshiba ⁶³
<u>Multijunction</u>							
InGaP/GaAs/InGaAs	31.2 ± 1.2	968 (da)	23.95	1.506	83.6	AIST (2/16)	Sharp (32 cells) ⁶⁴
<u>"Notable Exception"</u>							
CIGS (large)	18.6 ± 0.6	10 858 (ap)	58.00	4.545^b	76.8	FhG-ISE (10/19)	Miasole²⁸

(ap), aperture area; a-Si, amorphous silicon/hydrogen alloy; a-SiGe, amorphous silicon/germanium/hydrogen alloy; CIGSS, CuInGaSSe; (da), designated illumination area; Effic., efficiency; FF, fill factor; nc-Si, nanocrystalline or microcrystalline silicon; (t), total area.

^aSpectral response and current voltage curve reported in Version 49 of these tables.

^bSpectral response and current-voltage curve reported in the present version of these tables.

^cSpectral response and current-voltage curve reported in Version 50 or 51 of these tables.

^dStabilised at the manufacturer to the 2% level following IEC procedure of repeated measurements.

^eSpectral response and/or current-voltage curve reported in Version 46 of these tables.

^fInitial performance. References 7 and 8 review the stability of similar devices.

^gInitial performance. References 11 and 12 review the stability of similar devices.

^hSpectral response and current-voltage curve reported in Version 45 of these tables.

(readers identifying improved references are welcome to submit to the lead author). Table 1 summarises the best-reported measurements for "one-sun" (nonconcentrator) single-junction cells and submodules.

Table 2 contains what might be described as "notable exceptions" for "one-sun" single-junction cells and submodules in the above category. While not conforming to the requirements to be recognised as a class record, the devices in Table 2 have notable characteristics that will be of interest to sections of the photovoltaic community, with entries based on their significance and timeliness. To encourage discrimination, the table is limited to nominally 12 entries with the present authors having voted for their preferences for inclusion. Readers who have suggestions of notable exceptions for inclusion into this or subsequent tables are welcome to contact any of the authors with full details. Suggestions conforming to the guidelines will be included on the voting list for a future issue.

Table 3 was first introduced in Version 49 of these tables and summarises the growing number of cell and submodule results involving high efficiency, one-sun multiple-junction devices (previously reported in Table 1). Table 4 shows the best results for one-sun modules, both single-junction and multiple-junction, while Table 5 shows the best results for concentrator cells and concentrator modules. A small number of "notable exceptions" are also included in Tables 3–5.

2 | NEW RESULTS

Eighteen new results are reported in the present version of these tables. The first new result in Table 1 ("one-sun cells") is 23.2% efficiency for a large area (248-cm^2) cell fabricated upon an n-type directionally solidified (DS) wafer (commonly called a "cast mono" wafer), with the cell fabricated by Trina Solar and the result confirmed by the Institute für Solarenergieforschung (ISFH). A tunnelling polysilicon-oxide rear contacting (TOPCon) approach was used.⁴ The broader "DS wafer" category displaces the earlier "multicrystalline" category. Apart from challenges in defining and identifying multicrystallinity, to paraphrase a representative of one major wafer supplier,⁵ rather than the present competition being between monocrystalline and multicrystalline products, it is now between the ingot casting process (DS) and the Czochralski (CZ) growth process.

The second new result documents the ongoing progress with Pb-halide perovskite solar cells with 21.6% efficiency achieved for a 1-cm^2 cell fabricated by the Australian National University (ANU)⁶ and measured at a test centre newly recognised by the tables, the PV Performance Laboratory at the Australian Commonwealth Scientific, and Industrial Research Organisation (CSIRO). Measurements confirmed by CSIRO for perovskite solar cells are now eligible for inclusion in these tables (see Appendix for contact information). Along with other

TABLE 5 Terrestrial concentrator cell and module efficiencies measured under the ASTM G-173-03 direct beam AM1.5 spectrum at a cell temperature of 25°C

Classification	Effic., %	Area, cm ²	Intensity ^a , suns	Test Centre, Date	Description
<u>Single cells</u>					
GaAs	29.3 ± 0.7 ^b	0.09359 (da)	49.9	NREL (10/16)	LG Electronics
Si	27.6 ± 1.2 ^c	1.00 (da)	92	FhG-ISE (11/04)	Amonix back-contact ⁶⁵
CIGS (thin-film)	23.3 ± 1.2 ^{d,e}	0.09902 (ap)	15	NREL (3/14)	NREL ⁶⁶
<u>Multijunction cells</u>					
AlGaInP/AlGaAs/GaAs/GaInAs(3) (2.15/1.72/1.41/1.17/0.96/0.70 eV)	47.1 ± 2.6 ^{d,f}	0.099 (da)	143	NREL (3/19)	NREL, 6j inv. m'morphic ⁵⁹
GalnP/GaAs/GaInAsP/GaInAs	46.0 ± 2.2 ^g	0.0520 (da)	508	AIST (10/14)	Soitec/CEA/FhG-ISE 4j bonded ⁶⁷
GalnP/GaAs/GaInAs/GaInAs	45.7 ± 2.3 ^{d,h}	0.09709 (da)	234	NREL (9/14)	NREL, 4j monolithic ⁶⁸
InGaP/GaAs/InGaAs	44.4 ± 2.6 ⁱ	0.1652 (da)	302	FhG-ISE (4/13)	Sharp, 3j inverted metamorphic ⁶⁹
GalnAsP/GaInAs	35.5 ± 1.2 ^{j,d}	0.10031 (da)	38	NREL (10/17)	NREL 2-junction (2j) ⁷⁰
<u>Minimodule</u>					
GalnP/GaAs; GalnAsP/GaInAs	43.4 ± 2.4 ^{d,k}	18.2 (ap)	340 ^l	FhG-ISE (7/15)	Fraunhofer ISE 4j (lens/cell) ⁷¹
<u>Submodule</u>					
GalnP/GaInAs/Ge; Si	40.6 ± 2.0 ^k	287 (ap)	365	NREL (4/16)	UNSW 4j split spectrum ⁷²
<u>Modules</u>					
Si	20.5 ± 0.8 ^d	1875 (ap)	79	Sandia (4/89) ^m	Sandia/UNSW/ENTECH (12 cells) ⁷³
Three junction (3j)	35.9 ± 1.8 ⁿ	1092 (ap)	N/A	NREL (8/13)	Amonix ⁷⁴
Four junction (4j)	38.9 ± 2.5 ^o	812.3 (ap)	333	FhG-ISE (4/15)	Soitec ⁷⁵
<u>"Notable Exceptions"</u>					
Si (large area)	21.7 ± 0.7	20.0 (da)	11	Sandia (9/90) ^k	UNSW laser grooved ⁷⁶
Luminescent minimodule	7.1 ± 0.2	25(ap)	2.5 ^l	ESTI (9/08)	ECN Petten, GaAs cells ⁷⁷

(ap), aperture area; CIGS, CuInGaSe₂; (da), designated illumination area; Effic., efficiency; FhG-ISE, Fraunhofer-Institut für Solare Energiesysteme; NREL, National Renewable Energy Laboratory.

^aOne sun corresponds to direct irradiance of 1000 Wm⁻².

^bSpectral response and current-voltage curve reported in Version 50 of these tables.

^cMeasured under a low aerosol optical depth spectrum similar to ASTM G-173-03 direct⁷⁸.

^dNot measured at an external laboratory.

^eSpectral response and current-voltage curve reported in Version 44 of these tables.

^fSpectral response and current-voltage curve reported in Version 54 of these tables.

^gSpectral response and current-voltage curve reported in Version 45 of these tables.

^hSpectral response and current-voltage curve reported in Version 46 of these tables.

ⁱSpectral response and current-voltage curve reported in Version 42 of these tables.

^jSpectral response and current-voltage curve reported in Version 51 of these tables.

^kDetermined at IEC 62670-1 CSTC reference conditions.

^lGeometric concentration.

^mRecalibrated from original measurement.

ⁿReferenced to 1000 W/m² direct irradiance and 25°C cell temperature using the prevailing solar spectrum and an in-house procedure for temperature translation.

^oMeasured under IEC 62670-1 reference conditions following the current IEC power rating draft 62670-3.

emerging technologies, Pb-halide perovskite cells may not demonstrate the same level of stability as conventional cells, with the stability of such perovskite cells discussed elsewhere.⁷⁸ For the present device, the assigned efficiency was based on a "settled power at fixed voltage"

(SPFV) measurement where device voltage was held at the nominal maximum power point voltage of 1.05 V for 5 minutes.

Recent improvements documented in the tables for small-area organic photovoltaic (OPV) cell efficiency are now being reflected in

improved performance for larger area devices. An efficiency of 13.45% has been confirmed by the Fraunhofer Institute for Solar Energy Systems (FhG-ISE) for a 1-cm² OPV cell fabricated by the University of Potsdam.⁹ Similarly, an efficiency of 12.6% has been confirmed by FhG-ISE for a larger 26-cm² minimodule consisting of 12 serially connected cells submitted for certification by the Bavarian Centre for Applied Energy Research (ZAE), with involvement of the Friedrich-Alexander-Universität Erlangen-Nürnberg (FAU) and the Helmholtz Institute Erlangen-Nürnberg for Renewable Energy (HIERN), a branch of Forschungszentrum Jülich, in cooperation with South China University of Technology (SCUT).¹⁰ The module is based on solution-processed organic active materials using an “inverted” architecture (glass/ITO/ZnO nanoparticles/PM6:Y6:PCBM/MoO_x/Ag). The ternary bulk-heterojunction system comprises the donor polymer

“PM6 (PBDB-T-2F),” the nonfullerene acceptor molecule “Y6,” and the fullerene PC[60]BM. Devices are patterned by means of a 532-nm wavelength ns-laser. A slightly lower efficiency of 11.7% has also been confirmed by FhG-ISE for a much larger 204-cm² submodule consisting of 33 serially connected cells also submitted by ZAE Bayern using the same cell structure and patterning approach. As for perovskite cells, organic cells may not demonstrate the same level of stability as conventional cells, with the stability of these cells discussed elsewhere.^{11,12}

The first of six new results in Table 2 (one-sun “notable exceptions”) is an efficiency of 26.0% for a 4-cm² cell fabricated from 1 ohm cm p-type float-zone silicon with contacts on front and rear side. At the rear side the surface is passivated by a phosphorus doped polysilicon passivating contact (TOPCon) which also is the emitter of the solar cell. At the

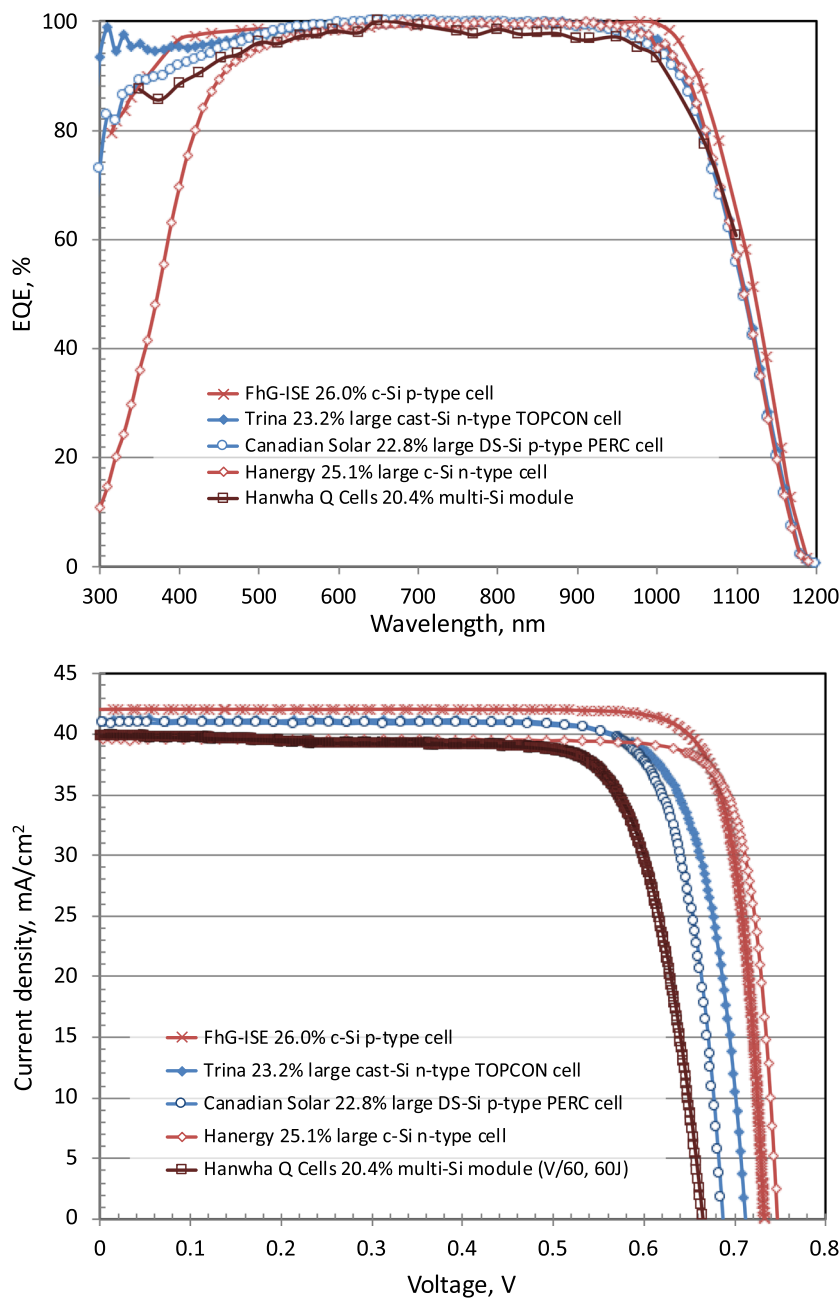


FIGURE 1 A, External quantum efficiency (EQE) for the Si cell and module results reported in this issue (some results may be normalised); B, corresponding current density–voltage (JV) curves [Colour figure can be viewed at wileyonlinelibrary.com]

front side the cell features a local boron diffusion underneath the contacts. The whole front side is passivated by a stack of Al₂O₃/SiNx/MgF. The cell was fabricated and measured by FhG-ISE.

The second new result is a total area efficiency of 25.1% reported for a large 244-cm² n-type silicon heterojunction (HJT) cell fabricated by Hanergy Thin Film Power Group, Chengdu, China¹³ and confirmed by ISFH. This efficiency is the highest reported for a large silicon cell with the two different polarity contacts on the opposite front and rear cell surfaces.

For the third new result in Table 2, ISFH confirmed 22.8% efficiency for a 247-cm² "multicrystalline P5" PERC cell on a p-type DS wafer fabricated by Canadian Solar with a "mono-cast" manufacturing process. High efficiency features include black-silicon texturing using Metal Catalysed Chemical Etch (MCCE), selective emitter, multilayer

antireflection coating, advanced surface passivation, and optimised grid and metallisation design.¹⁴

The fourth new result represents a new record for a Pb-halide perovskite solar cell, with an efficiency of 25.2% confirmed for a small area 0.1-cm² cell fabricated by the Korean Research Institute of Chemical Technology (KRICT) in conjunction with the Massachusetts Institute of Technology (MIT)¹⁵ and measured at the Newport PV Laboratory. Cell area is too small for classification as an outright record, with solar cell efficiency targets in governmental research programs generally specified in terms of a cell area of 1 cm² or larger.^{16–18}

The fifth new result in Table 2 represents a new record for a small-area (0.03-cm²) organic (OPV) cell with efficiency of 17.35%, arising from a collaboration between Shanghai Jiao Tong University (SJTU) and University of Massachusetts (UMass), Amherst and independently

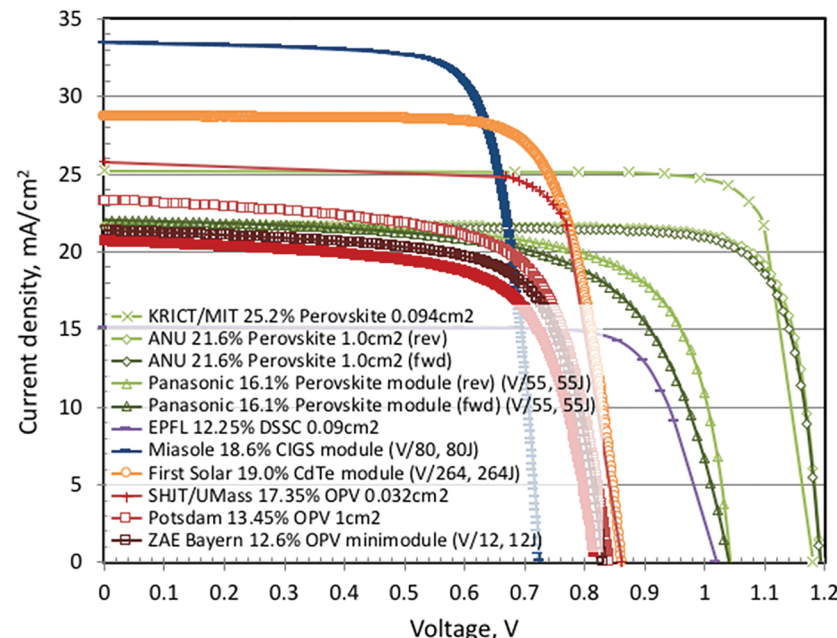
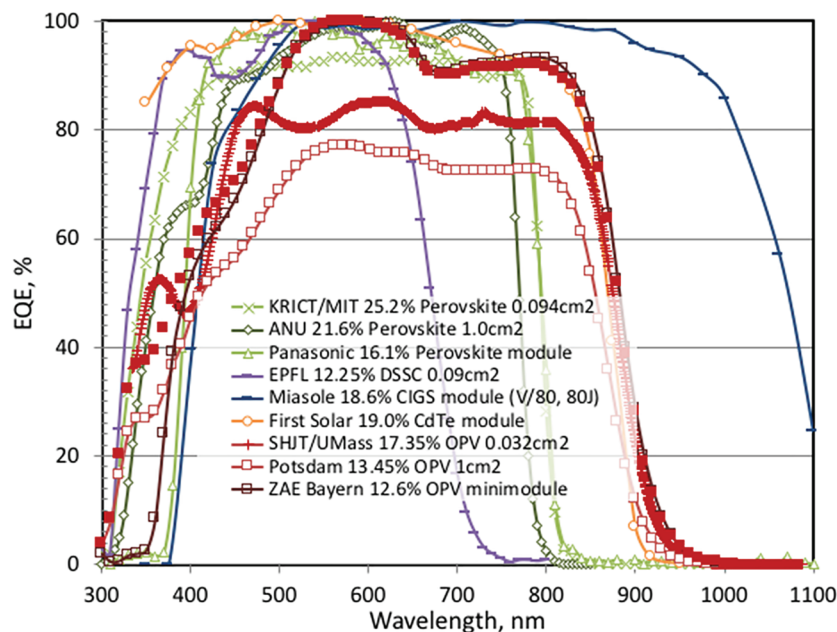


FIGURE 2 A, External quantum efficiency (EQE) for the thin film cell and module results reported in this issue (some results may be normalised); B, corresponding current density-voltage (JV) curves [Colour figure can be viewed at wileyonlinelibrary.com]

certified at the US National Renewable Energy Laboratory (NREL). An organic, four-component, solution-processed absorber layer was used, and the device stack was ITO/PEDOT:PSS/(organic layer)/PFNDI-BR/Al, as described elsewhere.¹⁹

The sixth new result recognises a slight improvement to 12.25% efficiency for a 0.1-cm² dye-sensitised cell fabricated by Ecole Polytechnique Fédérale de Lausanne (EPFL)²⁰ and again measured at the Newport PV Laboratory. Cell area is again too small for classification as an outright record. Along with other emerging technologies, dye-sensitised cells may not demonstrate the same level of stability as conventional cells, with the stability of these cells discussed elsewhere.²¹

Three new results are reported in Table 3 relating to one-sun, multijunction devices. Improvements are reported for two 4-cm² two-terminal, triple junction GaInP/(Al)GaAs/Si solar cells fabricated

and certified at FhG-ISE. In the first case, the silicon cell was wafer-bonded to the overlying III-V cell combination²² with a combined efficiency of 34.1%. In the second case, the cells were grown monolithically²³ giving an improvement in efficiency to 24.3%.

The third new result for Table 3 involves a 1-cm², two-terminal, monolithic perovskite/CIGSe double-junction cell with 23.3% efficiency fabricated by Helmholtz Zentrum Berlin (HZB)²⁴ and certified by FhG-ISE.

There are four very significant new entries in Table 4 ("one-sun modules"). The first is an efficiency of 20.4% for a large-area (1.5-m²) DS wafer silicon module fabricated by Hanwha Q Cells²⁵ and measured by FhG-ISE. This is the first DS wafer module to exceed 20% efficiency in these tables. The framed module dimensions are equivalent to the company's standard commercial product for modules containing 120 half-cells, although certification is based on the use of a slightly smaller

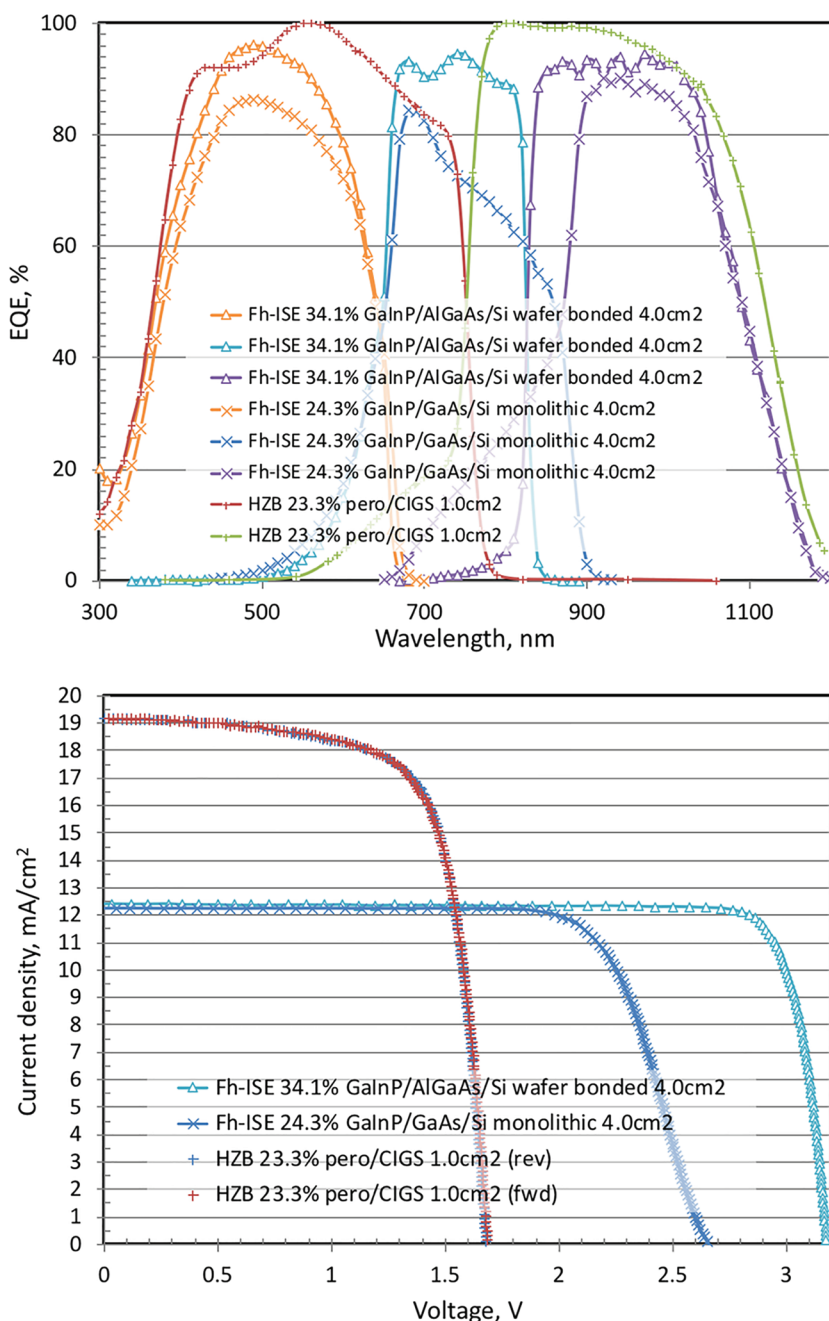


FIGURE 3 A, External quantum efficiency (EQE) for the multijunction cell results reported in this issue (some results may be normalised); B, corresponding current density-voltage (JV) curves [Colour figure can be viewed at wileyonlinelibrary.com]

area aperture mask, eliminating the inactive frame and outermost isolation areas from the measured module area.

The next new module result is 19.0% for a large-area (2.4-m^2) CdTe module fabricated by First Solar and again measured by FhG-ISE. In this case, the framed module dimensions are equivalent to the company's new, large-area "Series 6" module²⁶ containing "up to 264 cells," although certification is again based on the use of a slightly smaller area aperture mask, eliminating the inactive frame and outermost isolation areas from the measured area.

The third new result is 16.1% efficiency for a relatively small 802-cm^2 perovskite module fabricated by Panasonic and measured by the Japanese National Institute of Advanced Industrial Science and Technology (AIST). Earlier efforts by the same team reporting an unconfirmed module efficiency of 12.6% for an aperture area of 354 cm^2 are described elsewhere.²⁷

The final new entry in Table 4 as a "notable exception" is an efficiency of 18.6% for a large-area (1-m^2), flexible CIGS module fabricated by MiaSolé²⁸ and measured by FhG-ISE, improving on the company's earlier result.

The EQE spectra for the new silicon cell and module results reported in the present issue of these tables are shown in Figure 1A, with Figure 1B showing the current density-voltage (JV) curves for the same devices. Figure 2A,B shows the corresponding EQE and JV curves for the new thin film cell and module results, while Figure 3A, B shows these for the new multijunction cell results.

DISCLAIMER

While the information provided in the tables is provided in good faith, the authors, editors and publishers cannot accept direct responsibility for any errors or omissions.

ACKNOWLEDGMENT

The Australian Centre for Advanced Photovoltaics commenced operation in February 2013 with support from the Australian Government through the Australian Renewable Energy Agency (ARENA). The Australian Government does not accept responsibility for the views, information or advice expressed herein. The work at NREL was supported by the US Department of Energy under Contract No. DE-AC36-08-GO28308 with the National Renewable Energy Laboratory. The work at AIST was supported in part by the Japanese New Energy and Industrial Technology Development Organisation (NEDO) under the Ministry of Economy, Trade and Industry (METI).

ORCID

Martin A. Green  <https://orcid.org/0000-0002-8860-396X>
Anita W.Y. Ho-Baillie  <https://orcid.org/0000-0001-9849-4755>

REFERENCES

- Green MA, Hishikawa Y, Warta W, et al. Solar cell efficiency tables (Version 54). *Prog Photov: Res Appl.* 2019;27:565-575.
- Green MA, Hishikawa Y, Warta W, et al. Solar cell efficiency tables (Version 51). *Prog Photov: Res Appl.* 2018;26:3-12.
- Green MA, Emery K, Hishikawa Y, Warta W. Solar cell efficiency tables (Version 33). *Prog Photov: Res Appl.* 2009;17:85-94.
- <https://www.trinasolar.com/us/our-company> (accessed 11 November 2019).
- http://en.gcl-power.com/news_detail/2403-+New+Era+of+GCL+Cast+Mono+Silicon (Accessed 11 November 2019).
- <https://www.anu.edu.au/news/all-news/anu-researchers-set-solar-record-with-next-gen-cells> (accessed 28 October 2019)
- Han Y, Meyer S, Dkhissi Y, et al. Degradation observations of encapsulated planar $\text{CH}_3\text{NH}_3\text{PbI}_3$ perovskite solar cells at high temperatures and humidity. *J Mater Chem A.* 2015;8139-8147.
- Yang Y, You J. Make perovskite solar cells stable. *Nature.* 2017;544 (7649):155-156.
- <https://www.uni-potsdam.de/en/university-of-potsdam.html> (accessed 28 October, 2019)
- https://www.enccn.de/fileadmin/user_upload/PR_opv-record__.pdf (accessed 11 November, 2019)
- Tanenbaum DM, Hermenau M, Voroshazi E, et al. The ISOS-3 inter-laboratory collaboration focused on the stability of a variety of organic photovoltaic devices. *RSC Adv.* 2012;2:882-893.
- Krebs FC (Ed). Stability and degradation of organic and polymer solar cells. Wiley, Chichester, 2012; Jorgensen M, Norrman K, Gevorgyan SA, Tromholt T, Andreasen B, Krebs FC. Stability of polymer solar cells. *Adv Mater.* 2012;24:580-612.
- <http://taiyangnews.info/technology/24-23-shj-thin-film-conversion-efficiency-from-hanergy/> (accessed 28 October 2019).
- <http://investors.canadiansolar.com/news-releases/news-release-details/canadian-solar-sets-2280-conversion-efficiency-world-record-p> (accessed 27 October 2019).
- Jung EH, Jeon NJ, Park EY, et al. Efficient, stable and scalable perovskite solar cells using poly(3-hexylthiophene). *Nature.* 2019;567: 511-515.
- Program milestones and decision points for single junction thin films. *Annual Progress Report 1984, Photovoltaics, Solar Energy Research Institute, Report DOE/CE-0128, June 1985,* 7.
- Sakata I, Tanaka Y, Koizawa K. Japan's new national R&D program for photovoltaics. *Photovoltaic Energy Conversion, Conference Record of the 2006 IEEE 4th World Conference, Vol. 1, May 2008,* 1-4.
- Jäger-Waldau, A (Ed.). PVNET: European Roadmap for PV R&D, EUR 21087 EN, 2004.
- Li ZY, Ying L, Zhu P, et al. A generic green solvent concept boosting the power conversion efficiency of all-polymer solar cells to 11%. *Energ Environ Sci.* 2019;12:157-163.
- <https://www.epfl.ch/labs/lspm/>; <https://www.epfl.ch/labs/lpi/> (accessed 28 October 2019).
- Krašovec UO, Bokalič M, Topič M. Ageing of DSSC studied by electroluminescence and transmission imaging. *Solar Energy Materials and Solar Cells.* 2013;117:67-72.
- Cariou R, Benick J, Feldmann F, et al. III-V-on-silicon solar cells reaching 33% photoconversion efficiency in two-terminal configuration. *Nat Energy.* 2018;3(4):326-333. <https://doi.org/10.1038/s41560-018-0125-0>
- Feifel M, Lackner D, Ohlmann J, Benick J, Hermle M, Dimroth F. Direct growth of a GaInP/GaAs/Si triple-junction solar cell with 22.3% AM1.5 g efficiency. *Sol RRL.* 2019;1900313. <https://doi.org/10.1002/solr.201900313>
- <https://www.pv-magazine.com/2019/09/11/hzb-hits-23-26-efficiency-with-cigs-perovskite-tandem-cell/> (accessed 28 October 2019).
- <https://www.hanwha-qcells.com> (accessed 28 October 2019).

26. <http://www.firstsolar.com/en-AU/-/media/First-Solar/Technical-Documents/Series-6-Datasheets/Series-6-Datasheet.ashx> (accessed 28 October 2019).
27. Higuchi H, Negami T. Largest highly efficient 203 x 203 mm² CH₃NH₃PbI₃ perovskite solar modules. *Jpn J Appl Phys*. 2018;57:08RE11.
28. Bheemreddy V, Liu BJJ, Wills A, Murcia CP. Life prediction model development for flexible photovoltaic modules using accelerated damp heat testing. *IEEE 7th World Conference on Photovoltaic Energy Conversion (WCPEC)* 2018: 1249-1251.
29. Yoshikawa K, Kawasaki H, Yoshida W, et al. Silicon heterojunction solar cell with interdigitated back contacts for a photoconversion efficiency over 26%. *Nat Energy*. 2017;2:17032.
30. Moslehi MM, Kapur P, Kramer J, Rana V, Seutter S, Deshpande A, Stalcup T, Kommera S, Ashjaee J, Calcaterra A, Grupp D, Dutton D, Brown R. World-record 20.6% efficiency 156 mm x 156 mm full-square solar cells using low-cost kerfless ultrathin epitaxial silicon & porous silicon lift-off technology for industry-leading high-performance smart PV modules. *PV Asia Pacific Conference (APVIA/PVAP)*, 24 October 2012.
31. Keevers MJ, Young TL, Schubert U, Green MA. 10% efficient CSG minimodules. *22nd European Photovoltaic Solar Energy Conference*, Milan, September 2007.
32. Kayes BM, Nie H, Twist R, Spruytte SG, Reinhardt F, Kizilyalli IC, Higashi GS. 27.6% conversion efficiency, a new record for single-junction solar cells under 1 sun illumination. *Proceedings of the 37th IEEE Photovoltaic Specialists Conference*, 2011.
33. Venkatasubramanian R, O'Quinn BC, Hills JS, Sharps PR, Timmons ML, Hutchby JA, Field H, Ahrenkiel A, Keyes B. 18.2% (AM1.5) efficient GaAs solar cell on optical-grade polycrystalline Ge substrate. *Conference Record, 25th IEEE Photovoltaic Specialists Conference*, Washington, May 1997, 31-36.
34. Wanlass M. Systems and methods for advanced ultra-high-performance InP solar cells. US Patent 9,590,131 B2, 7 March 2017.
35. Nakamura M, Yamaguchi K, Kimoto Y, Yasaki Y, Kato T, Sugimoto H. Cd-free Cu (In,Ga)(Se,S)2 thin-film solar cell with a new world record efficiency of 23.35%, 46th IEEE PVSC, Chicago, IL, June 19, 2019. (see also http://www.solar-frontier.com/eng/news/2019/0117_press.html)
36. First Solar Press Release, First Solar builds the highest efficiency thin film PV cell on record, 5 August 2014.
37. https://en.dgist.ac.kr/site/dgist_eng/menu/984.do (accessed 28 October 2018).
38. Yan C, Huang J, Sun K, et al. Cu₂ZnSn S₄ solar cells with over 10% power conversion efficiency enabled by heterojunction heat treatment. *Nat Energy*. 2018;3:764-772.
39. Sai H, Matsui T, Kumagai H, Matsubara K. Thin-film microcrystalline silicon solar cells: 11.9% efficiency and beyond. *Applied Physics Express*. 2018;11:022301.
40. <http://www.microquanta.com> (accessed 9 May, 2018).
41. Komiya R, Fukui A, Murofushi N, Koide N, Yamanaka R and Katayama H. Improvement of the conversion efficiency of a monolithic type dye-sensitized solar cell module. *Technical Digest, 21st International Photovoltaic Science and Engineering Conference*, Fukuoka, November 2011; 2C-5O-08.
42. Kawai M. High-durability dye improves efficiency of dye-sensitized solar cells. *Nikkei Electronics* 2013; Feb.1 (http://techon.nikkeibp.co.jp/english/NEWS_EN/20130131/263532/) (accessed 23 October, 2013)
43. https://www.ise.fraunhofer.de/content/dam/ise/en/documents/annual_reports/fraunhofer-ise-annual-report-2018-2019.pdf (accessed 28 October 2018).
44. Richter A, Benick J, Feldmann F, Fell A, Hermle M, Glunz SW. n-Type Si solar cells with passivating electron contact: identifying sources for efficiency limitations by wafer thickness and resistivity variation. *Solar Energy Materials and Solar Cells*. 2017;173:96-105.
45. Haase F, Klamt C, Schäfer S, et al. Laser contact openings for local poly-Si-metal contacts enabling 26.1%-efficient POLO-IBC solar cells. *Solar Energy Materials and Solar Cells*. 2018;186:184-193.
46. NREL, private communication, 22 May 2019.
47. First Solar Press Release. First Solar achieves yet another cell conversion efficiency world record, 24 February 2016.
48. Wang W, Winkler MT, Gunawan O, et al. Device Characteristics of CZTSSe Thin-Film Solar Cells with 12.6% Efficiency. *Adv Energy Mater*. 2013. <https://doi.org/10.1002/aenm.201301465>
49. Sun K, Yan C, Liu F, et al. Beyond 9% efficient kesterite Cu₂ZnSnS₄ solar cell: fabricated by using Zn_{1-x}Cd_xS buffer layer. *Advanced Energy Materials*. 2016;6:1600046. <https://doi.org/10.1002/aenm.201600046>
50. Chiu PT, Law DL, Woo RL, Singer S, Bhusari D, Hong WD, Zakaria A, Boisvert JC, Mesropian S, King RR, Karam NH. 35.8% space and 38.8% terrestrial 5 J direct bonded cells. *Proc. 40th IEEE Photovoltaic Specialist Conference*, Denver, June 2014; 11-13.
51. Sasaki K, Agui T, Nakaido K, Takahashi N, Onitsuka R, Takamoto T. Proceedings, 9th International Conference on Concentrating Photovoltaics Systems, Miyazaki, Japan 2013.
52. Essig S, Allebé C, Remo T, et al. Raising the one-sun conversion efficiency of III-V/Si solar cells to 32.8% for two junctions and 35.9% for three junctions. *Nat Energy*. 2017;2(9):17144-17149. <https://doi.org/10.1038/nenergy.2017.144>
53. Grassman TJ, Chmielewski DJ, Carnevale SD, Carlin JA, Ringel SA. GaAs_{0.75}P_{0.25}/Si dual-junction solar cells grown by MBE and MOCVD. *IEEE J Photovoltaics*. 2016;6:326-331.
54. <https://www.oxfordpv.com/news/oxford-pv-perovskite-solar-cell-achieves-28-efficiency> (accessed 22/5/2019).
55. Green MA, Keevers MJ, Concha Ramon B, Jiang Y, Thomas I, Lasich JB, Verlinden PJ, Yang Y, Zhang X, Emery K, Moriarty T, King RR, Bensch W. Improvements in sunlight to electricity conversion efficiency: above 40% for direct sunlight and over 30% for global. Paper 1AP.1.2, *European Photovoltaic Solar Energy Conference 2015*, Hamburg, September 2015.
56. Sai H, Matsui T, Koida T, Matsubara K. Stabilized 14.0%-efficient triple-junction thin-film silicon solar cell. *Appl Phys Lett*. 2016;109:183506. <https://doi.org/10.1063/1.49669986>
57. Matsui T, Maejima K, Bidiville A, et al. High-efficiency thin-film silicon solar cells realized by integrating stable a-Si:H absorbers into improved device design. *Jpn J Appl Phys*. 2015;54:08KB10. <https://doi.org/10.7567/JJAP.54.08KB10>
58. <http://mldevices.com/index.php/news/> (accessed 28 October 2018).
59. Geisz JF, Steiner MA, Jain N, et al. Building a six-junction inverted metamorphic concentrator solar cell. *IEEE J Photovoltaics*. 2018;8:626-632.
60. Mattos LS, Scully SR, Syfu M, Olson E, Yang L, Ling C, Kayes BM, He G. New module efficiency record: 23.5% under 1-sun illumination using thin-film single-junction GaAs solar cells. *Proceedings of the 38th IEEE Photovoltaic Specialists Conference*, 2012.
61. Sugimoto H. High efficiency and large volume production of CIS-based modules. *40th IEEE Photovoltaic Specialists Conference*, Denver, June 2014.

62. Cashmore JS, Apolloni M, Braga A, et al. Improved conversion efficiencies of thin-film silicon tandem (MICROMORPH™) photovoltaic modules. *Solar Energy Materials and Solar Cells*. 2016;144:84–95. <https://doi.org/10.1016/j.solmat.2015.08.022>
63. Hosoya M, Oooka H, Nakao H, Gotanda T, Mori S, Shida N, Hayase R, Nakano Y, Saito M. Organic thin film photovoltaic modules. *Proceedings of the 93rd Annual Meeting of the Chemical Society of Japan* 2013; 21–37.
64. Takamoto, T. Application of InGaP/GaAs/InGaAs triple junction solar cells to space use and concentrator photovoltaic. *40th IEEE Photovoltaic Specialists Conference*, Denver, June 2014.
65. Slade A, Garboushian V. 27.6% efficient silicon concentrator cell for mass production. *Technical Digest, 15th International Photovoltaic Science and Engineering Conference*, Shanghai, October 2005, 701.
66. Ward JS, Ramanathan K, Hasoon FS, et al. A 21.5% efficient Cu (In,Ga) Se₂ thin-film concentrator solar cell. *Prog Photov: Res Appl*. 2002;10:41–46.
67. Dimroth F, Tibbets TND, Niemeyer M, Predan F, Beutel P, Karcher, C.; Oliva E, Siefer G, Lackner D, Fuß-Kailuweit P, Bett AW, Krause R, Drazek C, Guiot E, Wasselin J, Tauzin A, Signamarcheix T. Four-junction wafer-bonded concentrator solar cells. *IEEE J Photov* January 2016; 6(1): 343–349 <https://doi.org/10.1109/JPHOTOV.2015.2501729>
68. NREL Press Release NR-4514, 16 December 2014.
69. Press Release, Sharp Corporation, 31 May 2012 (accessed at <http://sharp-world.com/corporate/news/120531.htmlon5June2013>).
70. Jain N, Schulte KL, Geisz JF, et al. High-efficiency inverted metamorphic 1.7/1.1 eV GaInAsP/GaInAs dual-junction solar cells. *Appl Phys Lett*. 2018;112:053905.
71. Steiner M, Siefer G, Schmidt T, Wiesenfarth M, Dimroth F, Bett AW. 43 % sunlight to electricity conversion efficiency using CPV. *IEEE Journal of Photovoltaics* July. 2016;6(4):1020–1024. <https://doi.org/10.1109/JPHOTOV.2016.2551460>
72. Green MA, Keevers MJ, Thomas I, Lasich JB, Emery K, King RR. 40% efficient sunlight to electricity conversion. *Prog Photov: Res Appl*. 2015;23(6):685–691.
73. Chiang CJ and Richards EH. A 20% efficient photovoltaic concentrator module. *Conf. Record, 21st IEEE Photovoltaic Specialists Conference*, Kissimmee, May 1990: 861–863.
74. <http://amonix.com/pressreleases/amonix-achieves-world-record-359-module-efficiency-rating-nrel-4> (accessed 23 October 2013).
75. van Riesen S, Neubauer M, Boos A, Rico MM, Gourdel C, Wanka S, Krause R, Guernard P, Gombert A. New module design with 4-junction solar cells for high efficiencies. *Proceedings of the 11th Conference on Concentrator Photovoltaic Systems*, 2015.
76. Zhang F, Wenham SR, Green MA. Large area, concentrator buried contact solar cells. *IEEE Trans on Electron Devices*. 1995;42:144–149.
77. Slooff LH, Bende EE, Burgers AR, et al. A luminescent solar concentrator with 7.1% power conversion efficiency. *Phys Stat Sol (RRL)*. 2008;2 (6):257–259.
78. Gueymard CA, Myers D, Emery K. Proposed reference irradiance spectra for solar energy systems testing. *Solar Energy*. 2002;73:443–467.

How to cite this article: Green MA, Dunlop ED, Hohl-Ebinger J, Yoshita M, Kopidakis N, Ho-Baillie AWY. Solar cell efficiency tables (Version 55). *Prog Photovolt Res Appl*. 2020;28:3–15. <https://doi.org/10.1002/pip.3228>

APPENDIX A

UPDATE TO LIST OF DESIGNATED TEST CENTRES

A list of designated test centres is given in Version 51.² One addition is: Commonwealth Scientific & Industrial Research Organisation (CSIRO)

PV Performance Laboratory
10 Murray Dwyer Circuit, Mayfield West, NSW 2304, Australia
Contact: Dr Chris Fell
Phone: +61 (2) 4960 6000
Email: chris.fell@csiro.au
(perovskite solar cells)